

Higgs boson production in photon-photon collision at ILC: a comparative study in different little Higgs models

Lei Wang¹, Fuqiang Xu², Jin Min Yang³

¹ *Department of Physics, Yantai University, Yantai 264005, PR China*

² *Department of Physics, National Tsinghua University, Hsinchu, Taiwan 300, RO China*

³ *Key Laboratory of Frontiers in Theoretical Physics,
Institute of Theoretical Physics, Academia Sinica, Beijing 100190, PR China*

Abstract

We study the process $\gamma\gamma \rightarrow h \rightarrow b\bar{b}$ at ILC as a probe of different little Higgs models, including the simplest little Higgs model (SLH), the littlest Higgs model (LH), and two types of littlest Higgs models with T-parity (LHT-I, LHT-II). Compared with the Standard Model (SM) prediction, the production rate is found to be sizably altered in these little Higgs models and, more interestingly, different models give different predictions. We find that the production rate can be possibly enhanced only in the LHT-II for some part of the parameter space, while in all other cases the rate is suppressed. The suppression can be 10% in the LH and as much as 60% in both the SLH and the LHT-I/LHT-II. The severe suppression in the SLH happens for a large $\tan\beta$ and a small m_h , in which the new decay mode $h \rightarrow \eta\eta$ (η is a light pseudo-scalar) is dominant; while for the LHT-I/LHT-II the large suppression occurs when f and m_h are both small so that the new decay mode $h \rightarrow A_H A_H$ is dominant. Therefore, the precision measurement of such a production process at the ILC will allow for a test of these models and even distinguish between different scenarios.

PACS numbers: 14.80.Cp, 12.60.Fr, 14.70.Bh

I. INTRODUCTION

Little Higgs theory [1] has been proposed as an interesting solution to the hierarchy problem. So far various realizations of the little Higgs symmetry structure have been proposed [2–4], which can be categorized generally into two classes [5]. One class use the product group, represented by the littlest Higgs model (LH) [3], in which the SM $SU(2)_L$ gauge group is from the diagonal breaking of two (or more) gauge groups. The other class use the simple group, represented by the simplest little Higgs model (SLH) [4], in which a single larger gauge group is broken down to the SM $SU(2)_L$. However, due to the tree-level mixing of heavy and light mass eigenstates, the electroweak precision tests can give strong constraints on this model [6–8], which would require raising the mass scale of new particles to be much higher than TeV and thus reintroduce the fine-tuning in the Higgs potential. To tackle this problem, a discrete symmetry called T-parity is proposed [9], which forbids those tree-level contributions to the electroweak observables. For the LH, there are two different versions of implementing T-parity in the top quark Yukawa interaction. In the pioneer version of this model (hereafter called LHT-I) [10], the T-parity is simply implemented by adding the T-parity images for the original top quark interaction to make the Lagrangian T-invariant. A characteristic prediction of this model is a T-even top partner which cancels the Higgs mass quadratic divergence contributed by the top quark. An alternative implementation of T-parity has been proposed (hereafter called LHT-II) [11], where all new particles including the heavy top partner responsible for cancelling the SM one-loop quadratic divergence are odd under T-parity. The implementation of T-parity in the SLH model has also been tried [12].

These little Higgs models mainly alter the property of the Higgs boson and hence the hints of these models can be unravelled from various Higgs boson processes. The Higgs decay and main production channels at the LHC have been studied in the SLH [13–16], the LH [13, 17, 18], and the LHT-I [19, 20] and LHT-II [21]. While the LHC is widely regarded as a discovery machine for Higgs boson and also could possibly allow for a measurement of decay partial widths at 10% – 30% level [22], a precision measurement of Higgs property can be only achieved at the proposed International Linear Collider (ILC). With the ILC, the Higgs nature can be scrutinized through the production in photon-photon collision, where the photon beam can be obtained by backscattering a laser light with high energy e^\pm

beam. Such an option of photon-photon collision can possibly measure the rates of Higgs productions with a precision of a few percent. Especially, for $\gamma\gamma \rightarrow h \rightarrow b\bar{b}$ process, the production rate could be measured at about 2% for a light Higgs boson [23, 24].

Such a process $\gamma\gamma \rightarrow h \rightarrow b\bar{b}$ is a sensitive probe for new physics because both the loop-induced $h\gamma\gamma$ coupling and the $hb\bar{b}$ coupling are sensitive to new physics. Considering the sizable alteration of Higgs couplings in various little Higgs models, we in this work study the process $\gamma\gamma \rightarrow h \rightarrow b\bar{b}$ as a probe of different little Higgs models, including the SLH, LH, LHT-I and LHT-II. Note that this process has been studied in the LH [25] and also in the SLH [15]. In our study we give a comprehensive and comparative analysis for all these models. In addition, since a recent study of Z leptonic decay gave a new stronger bound on the parameter f in the SLH [8], we will consider such a new bound in our calculation for the SLH.

This work is organized as follows. In Sec. II we recapitulate the models. In Sec. III we calculate the rate of $\gamma\gamma \rightarrow h \rightarrow b\bar{b}$ in these models. Finally, we give our conclusion in Sec. IV.

II. LITTLE HIGGS MODELS

A. Simplest little Higgs model

The SLH [4] model is based on $[SU(3) \times U(1)_X]^2$ global symmetry. The gauge symmetry $SU(3) \times U(1)_X$ is broken down to the SM electroweak gauge group by two copies of scalar fields Φ_1 and Φ_2 , which are triplets under the $SU(3)$ with aligned VEVs f_1 and f_2 . The uneaten five pseudo-Goldstone bosons can be parameterized as

$$\Phi_1 = e^{i t_\beta \Theta} \begin{pmatrix} 0 \\ 0 \\ f_1 \end{pmatrix}, \quad \Phi_2 = e^{-i t_\beta \Theta} \begin{pmatrix} 0 \\ 0 \\ f_2 \end{pmatrix}, \quad (1)$$

where

$$\Theta = \frac{1}{f} \left[\begin{pmatrix} 0 & 0 & H \\ 0 & 0 & \\ H^\dagger & 0 & \end{pmatrix} + \frac{\eta}{\sqrt{2}} \begin{pmatrix} 1 & 0 & 0 \\ 0 & 1 & 0 \\ 0 & 0 & 1 \end{pmatrix} \right], \quad (2)$$

with $f = \sqrt{f_1^2 + f_2^2}$ and $t_\beta \equiv \tan\beta = f_2/f_1$. Under the SM $SU(2)_L$ gauge group, η is a singlet CP-odd scalar, while H transforms as a doublet and can be identified as the SM Higgs doublet. The other five Goldstones are eaten by new gauge bosons Z' , $W'_{0,0}$, and W'^{\pm} , which obtain masses proportional to f :

$$m_{W'^+}^2 = \frac{g^2}{2}f^2, \quad m_{W'^0}^2 = \frac{g^2}{2}f^2, \quad m_{Z'}^2 = g^2f^2 \frac{2}{3 - \tan^2\theta_W}, \quad (3)$$

with θ_W being the electroweak mixing angle.

The gauged $SU(3)$ symmetry promotes the SM fermion doublets into $SU(3)$ triplets. There are two possible gauge charge assignments for the fermions: the 'universal' embedding and the 'anomaly-free' embedding. Since the first choice is not favored by the electroweak precision data [4], we focus on the second way of embedding. The top, strange, and down quarks have heavy partner quarks T , S , and D , respectively. The mixing between light quarks and heavy partners can be parameterized by

$$x_\lambda^t \equiv \frac{\lambda_1^t}{\lambda_2^t}, \quad x_\lambda^d \equiv \frac{\lambda_1^d}{\lambda_2^d}, \quad x_\lambda^s \equiv \frac{\lambda_1^s}{\lambda_2^s}. \quad (4)$$

To leading order, the heavy partners have masses proportional to f :

$$m_Q = \sqrt{(\lambda_1^q c_\beta)^2 + (\lambda_2^q s_\beta)^2} f, \quad (5)$$

where $Q = T, D, S$; $q = t, d, s$; $c_\beta = \frac{f_1}{\sqrt{f_1^2 + f_2^2}}$, $s_\beta = \frac{f_2}{\sqrt{f_1^2 + f_2^2}}$; λ_1^q and λ_2^q are two dimensionless couplings of q -quark Yukawa sector.

The Yukawa and gauge interactions break the global symmetry and then provide a potential for the Higgs boson. However, the Coleman-Weinberg potential alone is not sufficient since the generated Higgs mass is too heavy and the new CP-odd scalar η is massless. Therefore, one can introduce a tree-level μ term which can partially cancel the Higgs mass

$$-\mu^2(\Phi_1^\dagger \Phi_2 + h.c.) = -2\mu^2 f^2 s_\beta c_\beta \cos\left(\frac{\eta}{\sqrt{2}s_\beta c_\beta f}\right) \cos\left(\frac{\sqrt{H^\dagger H}}{f c_\beta s_\beta}\right). \quad (6)$$

Then the scalar potential becomes

$$V = -m^2 H^\dagger H + \lambda(H^\dagger H)^2 - \frac{1}{2}m_\eta^2 \eta^2 + \lambda' H^\dagger H \eta^2 + \dots, \quad (7)$$

where

$$m^2 = m_0^2 - \frac{\mu^2}{s_\beta c_\beta}, \quad \lambda = \lambda_0 - \frac{\mu^2}{12s_\beta^3 c_\beta^3 f^2}, \quad \lambda' = -\frac{\mu^2}{4f^2 s_\beta^3 c_\beta^3}, \quad (8)$$

with m_0 and λ_0 being respectively the one-loop contributions to the Higgs boson mass and the quartic couplings from the contributions of fermion loops and gauge boson loops [4]. The Higgs VEV, the Higgs boson mass and the mass of η are given by

$$v^2 = \frac{m^2}{\lambda}, \quad m_h^2 = 2m^2, \quad m_\eta^2 = \frac{\mu^2}{s_\beta c_\beta} \cos\left(\frac{v}{\sqrt{2}f s_\beta c_\beta}\right). \quad (9)$$

The Coleman-Weinberg potential involves the following parameters:

$$f, \quad x_\lambda^t, \quad t_\beta, \quad \mu, \quad m_\eta, \quad m_h, \quad v. \quad (10)$$

Due to the modification of the observed W -boson mass, v is defined as [14]

$$v \simeq v_{SM} \left[1 + \frac{v_{SM}^2}{12f^2} \frac{t_\beta^4 - t_\beta^2 + 1}{t_\beta^2} - \frac{v_{SM}^4}{180f^4} \frac{t_\beta^8 - t_\beta^6 + t_\beta^4 - t_\beta^2 + 1}{t_\beta^4} \right], \quad (11)$$

where $v_{SM} = 246$ GeV is the SM Higgs VEV. Assuming that there are no large direct contributions to the potential from physics at the cutoff, we can determine other parameters in Eq. (10) from f , t_β and m_h with the definition of v in Eq. (11).

B. Littlest Higgs model

The LH model [3, 26] is based on a non-linear σ model in the coset space of $SU(5)/SO(5)$ with additional local gauge symmetry $[SU(2) \otimes U(1)]^2$. A VEV of an $SU(5)$ symmetric tensor field breaks the $SU(5)$ to $SO(5)$ at the scale f with

$$\Sigma_0 = \begin{pmatrix} 0 & 0 & \mathbb{1} \\ 0 & 1 & 0 \\ \mathbb{1} & 0 & 0 \end{pmatrix}. \quad (12)$$

The non-linear sigma fields are then parameterized by the Goldstone fluctuations as

$$\Sigma \simeq \Sigma_0 + \frac{2i}{f} \begin{pmatrix} \phi^\dagger & \frac{H^\dagger}{\sqrt{2}} & \mathbf{0}_{2 \times 2} \\ \frac{H^*}{\sqrt{2}} & 0 & \frac{H}{\sqrt{2}} \\ \mathbf{0}_{2 \times 2} & \frac{H^T}{\sqrt{2}} & \phi \end{pmatrix} + \mathcal{O}\left(\frac{1}{f^2}\right), \quad (13)$$

where H is a doublet and ϕ is a triplet under the unbroken $SU(2)_L$. The other four Goldstones are eaten by new gauge bosons W_H^\pm , Z_H , and A_H , which get masses of order f :

$$m_{Z_H} = m_{W_H} = \frac{gf}{2sc}, \quad m_{A_H} = \frac{g'f}{2\sqrt{5}s'c'}, \quad (14)$$

with c , s , c' and s' being the mixing parameters in the gauge boson sector given by

$$\begin{aligned} c \equiv \cos \theta &= \frac{g_1}{\sqrt{g_1^2 + g_2^2}}, & s \equiv \sin \theta &= \frac{g_2}{\sqrt{g_1^2 + g_2^2}}, \\ c' \equiv \cos \theta' &= \frac{g'_1}{\sqrt{g_1'^2 + g_2'^2}}, & s' \equiv \sin \theta' &= \frac{g'_2}{\sqrt{g_1'^2 + g_2'^2}}. \end{aligned} \quad (15)$$

Here g_j and g'_j are the $SU(2)_j$ and $U(1)_j$ ($j = 1, 2$) gauge coupling constants, respectively.

The top quark loops, gauge boson loops and scalar particles loops can generate the Higgs potential, which trigger electroweak symmetry breaking. The heavy bosons can further mix with light bosons, leading the masses of heavy and light gauge bosons corrected at $\mathcal{O}(\frac{v^2}{f^2})$. The components Φ^{++} , Φ^+ , Φ^0 and Φ^P (neutral pseudo-scalar) of the triplet ϕ get a mass

$$m_\Phi = \frac{\sqrt{2}m_h}{\sqrt{1-x^2}} \frac{f}{v}, \quad (16)$$

where x is a free parameter of the Higgs sector proportional to the triplet VEV v' and defined as $x = \frac{4fv'}{v^2}$ with v being the LH Higgs VEV given by [18]

$$v \simeq v_{SM} [1 - \frac{v_{SM}^2}{f^2} (-\frac{5}{24} + \frac{1}{8}x^2)]. \quad (17)$$

In the fermion sector, there is an extra top quark partner T -quark, which cancels the Higgs mass one-loop quadratic divergence contributed by the top quark. The mixing between t and T can be parameterized by

$$r = \frac{\lambda_1}{\lambda_2}, \quad c_t = \frac{1}{\sqrt{r^2 + 1}}, \quad s_t = \frac{r}{\sqrt{1 + r^2}}, \quad (18)$$

where λ_1 and λ_2 are two dimensionless couplings of top quark Yukawa sector. Together with f , the parameters can control the T -quark mass

$$m_T = \frac{m_t f}{s_t c_t v}. \quad (19)$$

C. Littlest Higgs models with T-parity

In the LHT-I [10, 19, 27], the T-parity is simply implemented by adding the T-parity images for the original top quark interaction to make the Lagrangian T-invariant. A characteristic prediction of this model is a T-even top partner which cancels the Higgs mass quadratic divergence contributed by the top quark. Inspired by the way that the top quadratic divergence is cancelled in the SLH, Ref. [11] takes an alternative implementation of T-parity in

LHT-II, where all new particles including the heavy top partner responsible for cancelling the SM one-loop quadratic divergence are odd under T-parity. Thus, Higgs couplings with top quark and partners in the two models have sizable difference. Besides, for each SM quark (lepton), a copy of mirror quark (lepton) with T-odd quantum number is added in order to preserve the T-parity. The Higgs couplings with the down-type T-odd fermions are absent, and the couplings with the up-type T-odd fermions are different in LHT-I and LHT-II. For the above reasons, LHT-I and LHT-II can give distinct predictions for production rates of single Higgs, Higgs-pair, as well as a Higgs boson associated with a pair of top and anti-top quarks at LHC [21].

For the SM down-type quarks (leptons), the Higgs couplings have two different cases [19]

$$\begin{aligned}\frac{g_{hdd}}{g_{hdd}^{\text{SM}}} &\simeq 1 - \frac{1}{4} \frac{v_{SM}^2}{f^2} + \frac{7}{32} \frac{v_{SM}^4}{f^4} && \text{for Case A,} \\ &\simeq 1 - \frac{5}{4} \frac{v_{SM}^2}{f^2} - \frac{17}{32} \frac{v_{SM}^4}{f^4} && \text{for Case B.}\end{aligned}$$

The relation of down-type quark couplings also applies to the lepton couplings.

The LHT-I and LHT-II have the same kinetic term of Σ field where the T-parity can be naturally implemented by setting $g_1 = g_2$ and $g'_1 = g'_2$. Under T-parity, the SM bosons are T-even and the new bosons are T-odd. Therefore, the coupling of $H^\dagger \phi H$ is forbidden, leading the triplet VEV $v' = 0$. In both LHT-I and LHT-II, the Higgs VEV v is modified as [19, 21]

$$v \simeq v_{SM} \left(1 + \frac{1}{12} \frac{v_{SM}^2}{f^2} \right). \quad (20)$$

III. THE PROCESS $\gamma\gamma \rightarrow h \rightarrow b\bar{b}$ IN LITTLE HIGGS MODELS

A. Calculations

We consider a photon-photon collision at the ILC with the photon beams obtained by Compton backscattering of lasers from the e^\pm beams. The cross section $\sigma(\gamma\gamma \rightarrow h)$ at the ILC is obtained by folding the cross section $\hat{\sigma}_{\gamma\gamma \rightarrow h}(\hat{s})$ with the photon luminosity

$$\sigma(\gamma\gamma \rightarrow h) = \int_0^1 d\tau \int_\tau^1 \frac{dx}{x} f_{\gamma/e}(x) f_{\gamma/e}(\tau/x) \hat{\sigma}_{\gamma\gamma \rightarrow h}(\hat{s}), \quad (21)$$

where $f_{\gamma/e}(x)$ is the energy spectrum of the back-scattered photon [28]. The cross section $\hat{\sigma}$ is given by

$$\hat{\sigma}_{\gamma\gamma\rightarrow h}(\hat{s}) = \frac{8\pi^2}{m_h} \Gamma(h \rightarrow \gamma\gamma) \delta(\hat{s} - m_h^2), \quad (22)$$

where $\hat{s} = \tau s$ with \sqrt{s} being the center-of-mass energy of the ILC. The rate of $\gamma\gamma \rightarrow h \rightarrow b\bar{b}$ can be approximately obtained by $\sigma(\gamma\gamma \rightarrow h) \times BR(h \rightarrow b\bar{b})$. So, we need to calculate both the production cross section $\sigma(\gamma\gamma \rightarrow h)$ and the decay widths.

Now we discuss the Higgs decays in little Higgs models. For the tree-level decays $h \rightarrow f\bar{f}$ (SM fermion pair), WW and ZZ , the little Higgs models give the correction via the corresponding modified couplings

$$\Gamma(h \rightarrow XX) = \Gamma(h \rightarrow XX)_{SM} (g_{hXX}/g_{hXX}^{SM})^2, \quad (23)$$

where XX denotes WW , ZZ or fermion pairs, $\Gamma(h \rightarrow XX)_{SM}$ is the SM decay width, and g_{hXX} and g_{hXX}^{SM} are the couplings of hXX in the little Higgs models and SM, respectively.

The loop-induced decay $h \rightarrow gg$ will be also important for a low Higgs mass. The effective coupling of hgg is presented in Appendix A. In the SM, the main contributions are from the top quark loop, and the little Higgs models give the corrections via the modified couplings $ht\bar{t}$. In addition, the decay width of $h \rightarrow gg$ can be also corrected by the loops of heavy partner quark T , D and S in SLH (T quark in LH) (new T-even and T-odd quarks in LHT-I and LHT-II).

For the decay $h \rightarrow \gamma\gamma$, the main contributions are from the top quark loop and W -boson loop in the SM. The little Higgs models give the corrections via the modified couplings $ht\bar{t}$ and hWW . In these models the new quarks which contribute to the decay $h \rightarrow gg$ also contribute to the decay $h \rightarrow \gamma\gamma$. In addition to the contributions from fermion loops, the decay width of $h \rightarrow \gamma\gamma$ can be also corrected by the loops of W' in the SLH (W_H , Φ^+ , Φ^{++} in the LH, LHT-I and LHT-II). The effective coupling of $h\gamma\gamma$ can be found in Appendix A.

In addition to the SM decay modes, the Higgs boson in the SLH, LHT-I and LHT-II has some new important decay modes which are kinematically allowed in the parameter space. In the SLH, the new decay modes are $h \rightarrow \eta\eta$ and $h \rightarrow Z\eta$, whose partial widths are given by

$$\begin{aligned} \Gamma(h \rightarrow \eta\eta) &= \frac{\lambda'^2 v^2}{8\pi m_h} \sqrt{1 - x_\eta}, \\ \Gamma(h \rightarrow Z\eta) &= \frac{m_h^3}{32\pi f^2} \left(t_\beta - \frac{1}{t_\beta}\right)^2 \lambda^{3/2} \left(1, \frac{m_Z^2}{m_h^2}, \frac{m_\eta^2}{m_h^2}\right), \end{aligned} \quad (24)$$

where $x_\eta = 4m_\eta^2/m_h^2$ and $\lambda(1, x, y) = (1 - x - y)^2 - 4xy$. In the LHT-I and LHT-II, the new decay mode is $h \rightarrow A_H A_H$, whose partial width is

$$\Gamma(h \rightarrow A_H A_H) = \frac{g_{hA_H A_H}^2 m_h^3}{128\pi m_{A_H}^4} \sqrt{1 - x_{A_H}} \left(1 - x_{A_H} + \frac{3}{4} x_{A_H}^2 \right), \quad (25)$$

where $x_{A_H} = 4m_{A_H}^2/m_h^2$, and $g_{hA_H A_H}$ is the coupling constants of $hA_H A_H$. Note that the breaking scale f in LHT-I may be as low as 500 GeV [29], and the constraint in LHT-II is expected to be even weaker [11]. Therefore, for a lower value of f , the lightest T-odd particle A_H may have a light mass, $m_{A_H} < \frac{m_h}{2}$, leading to the decay $h \rightarrow A_H A_H$. However, in the LH the electroweak precision data requires f larger than a few TeV [6] and thus the decay $h \rightarrow A_H A_H$ is kinematically forbidden.

In our calculations, the SM input parameters involved are taken from [30]. For the SM decay channels, the relevant higher order QCD and electroweak corrections are considered using the code Hdecay [31]. In the SLH, the new free parameters are f , t_β , $x_\lambda^d (m_D)$ and $x_\lambda^s (m_S)$. As shown above, the parameters x_λ^t , μ , m_η can be determined by f , t_β , m_h and v . The small mass of the d (s) quark requires one of the couplings λ_1^d and λ_2^d (λ_1^s and λ_2^s) to be very small, so there is almost no mixing between the SM down-type quarks and their heavy partners. We assume λ_1^d (λ_1^s) is small, and take $x_\lambda^d = 1.1 \times 10^{-4}$ ($x_\lambda^s = 2.1 \times 10^{-3}$), which can make the masses of D and S in the range of 1-2 TeV with other parameters fixed as in our calculation. In fact, our results show that the contributions from d and D (s and S) are very small compared with the effects from t and T . The electroweak precision data can give a strong constraint on the scale f . Ref.[4] shows that the LEP-II data requires $f > 2$ TeV. In addition, the contributions to the electroweak precision data can be suppressed by large t_β . Ref. [7] gives a lower bound of $f > 4.5$ TeV from the oblique parameter S , while a recent study of Z leptonic decay gives a stronger bound of $f > 5.6$ TeV [8]. Considering the above bounds, in our numerical calculation we will take several values of t_β for $f = 2$ TeV, $f = 4$ TeV and $f = 5.6$ TeV.

In the LH model, the new free parameters involved are f , $c_t (r)$, c , c' and x , where

$$0 < c_t < 1, \quad 0 < c < 1, \quad 0 < c' < 1, \quad 0 < x < 1. \quad (26)$$

Taking $f = 1$ TeV, $f = 2$ TeV and $f = 4$ TeV, we will scan over these parameters in the above ranges and show the scatter plots. Note that the widths $\Gamma(h \rightarrow t\bar{t})$, $\Gamma(h \rightarrow gg)$ and $\Gamma(h \rightarrow \gamma\gamma)$ involve the parameter c_t which can control Higgs couplings with t , T and m_T .

For a light Higgs boson, the decay mode $h \rightarrow t\bar{t}$ is kinematically forbidden. For the decay $\Gamma(h \rightarrow gg)$ and $\Gamma(h \rightarrow \gamma\gamma)$, the c_t dependence of top-quark loop can cancel that of T-quark loop to a large extent [25]. Therefore, the rate $\sigma(\gamma\gamma \rightarrow h) \times BR(h \rightarrow b\bar{b})$ is not sensitive to c_t for a light Higgs boson.

In LHT-I and LHT-II, the parameters c , c' and x are fixed as

$$c = c' = \frac{1}{\sqrt{2}}, \quad x = 0. \quad (27)$$

The heavy T-even and T-odd quarks only have large contributions to the decay widths of $h \rightarrow gg$ and $h \rightarrow \gamma\gamma$, which are not sensitive to the actual values of their masses as long as they are much larger than half of the Higgs boson mass [18]. Similar to the LH model, the result is not sensitive to c_t in LHT-I and LHT-II. Taking $c_t = 1/\sqrt{2}$ ($\lambda_1 = \lambda_2$) can simplify the top quark Yukawa sector in the LHT-II [11, 21], and this choice is also favored by the electroweak precision data [29]. Therefore, in our numerical calculations we take $c_t = 1/\sqrt{2}$.

B. Discussions

The numerical results for the rate $\sigma(\gamma\gamma \rightarrow h) \times BR(h \rightarrow b\bar{b})$ are shown in Figs. 1, 2 and 3, normalized to the SM prediction. We see that the rate in all these little Higgs models can have a sizable deviation from the SM prediction, and the magnitude of deviation is sensitive to the scale f .

Fig. 1 shows that the SLH model always suppresses the rate, and the suppression is more sizable for a large $\tan\beta$. When $\tan\beta$ is large enough, such as $t_\beta = 10$ for $f = 2$ TeV ($t_\beta = 18$ for $f = 4$ TeV or $t_\beta = 25$ for $f = 5.6$ TeV), the suppression can be as much as 90%. The reason for such a severe suppression is that the decay mode $h \rightarrow \eta\eta$ can be dominant in some part of the parameter space and thus the total decay width of Higgs boson becomes much larger than the SM value. Note that $\tan\beta$ cannot be too large for a fixed f in order for the perturbation to be valid. As shown in Eq. (11), the correction to the Higgs VEV is proportional to $\tan^2\beta v_{SM}^2/f^2$. If we require $\mathcal{O}(v_{SM}^4/f^4)/\mathcal{O}(v_{SM}^2/f^2) < 0.1$ in the expansion of v , the value of $\tan\beta$ should be below 10, 20, and 28 for $f = 2$ TeV, 4 TeV, and 5.6 TeV, respectively.

Fig. 2 shows that the LH model also always suppresses the rate $\sigma(\gamma\gamma \rightarrow h) \times BR(h \rightarrow b\bar{b})$, but the suppression can only reach about 10%. For a light Higgs boson or a large value of

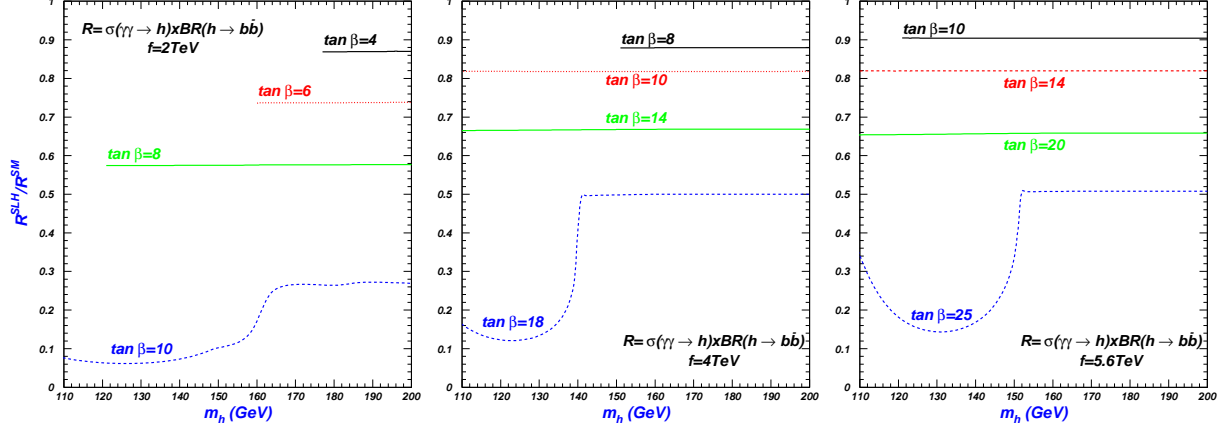


FIG. 1: The rate $\sigma(\gamma\gamma \rightarrow h) \times BR(h \rightarrow b\bar{b})$ normalized to the SM prediction in the SLH model. The incomplete lines for small values of $\tan\beta$ show the lower bounds of Higgs mass.

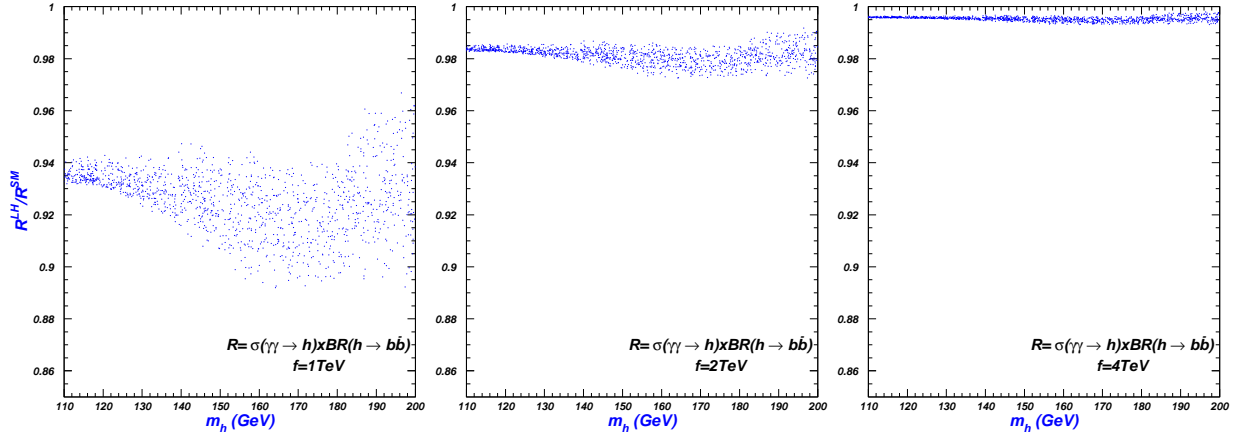


FIG. 2: Scatter plots for the rate $\sigma(\gamma\gamma \rightarrow h) \times BR(h \rightarrow b\bar{b})$ normalized to the SM prediction in the LH model.

f , the suppression is small and not sensitive to the parameters c , c' , c_t and x . For example, for $f = 2$ TeV the suppression is only a few percent.

Fig. 3 shows that LHT-I always suppresses the rate but LHT-II can either suppress or enhance the rate, depending on the values of the Higgs mass and scale f . For each model the rate in Case A is always above the rate in Case B because the $h b\bar{b}$ coupling in Case A is less suppressed than in Case B. Also, we see that for $f = 500$ GeV and m_h in the range of $130 - 150$ GeV, the rate in both models drops drastically. The reason for such a severe suppression is similar to what happens in the SLH model discussed above, i.e., the opening of new decay mode (but now the new mode is $h \rightarrow A_H A_H$).

From our above results we see that the Higgs production process $\gamma\gamma \rightarrow h \rightarrow b\bar{b}$ can be a powerful probe for various little Higgs models. Also, as shown in the literature [32], the

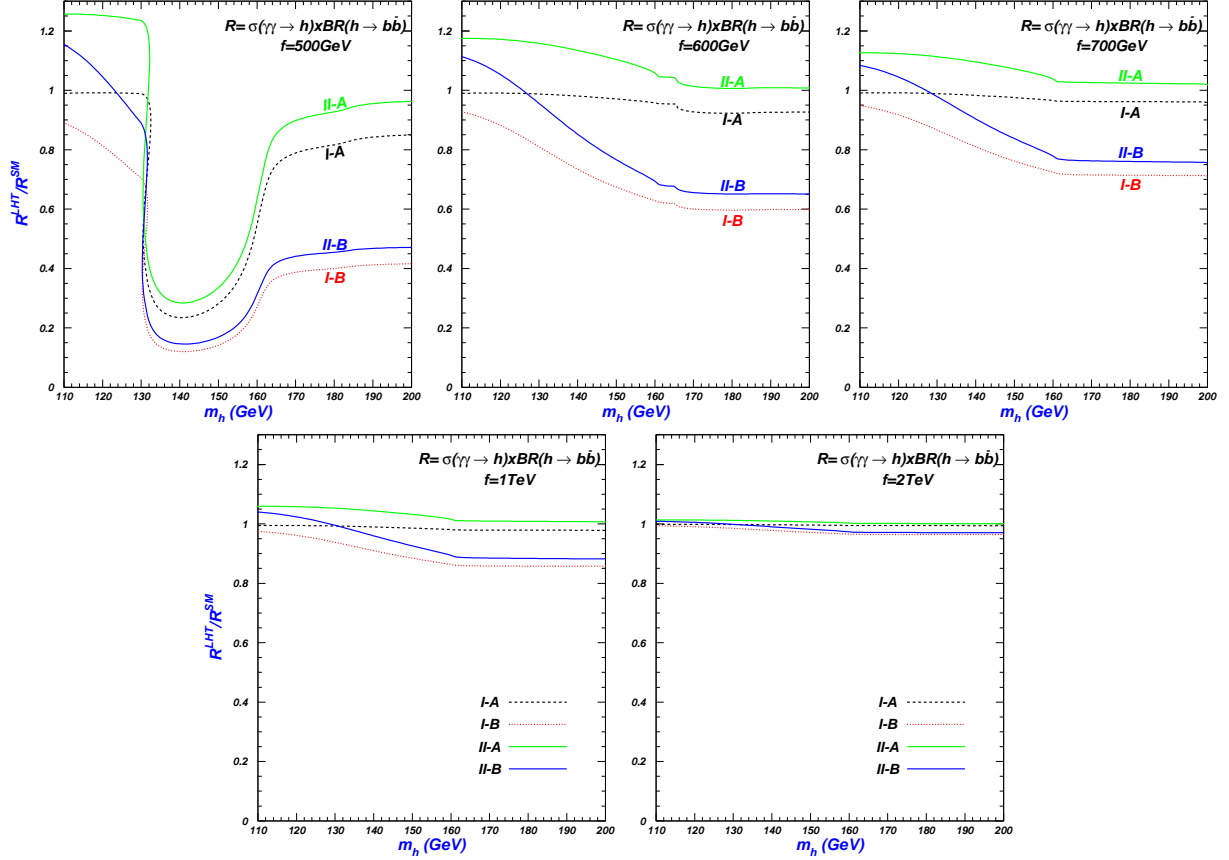


FIG. 3: The rate $\sigma(\gamma\gamma \rightarrow h) \times BR(h \rightarrow b\bar{b})$ normalized to the SM prediction in the LHT-I and LHT-II models. Here I-A (II-A) and I-B (II-B) denote Case A and Case B, respectively.

photon-photon collision option of the ILC can probe the top-quark related new physics more effectively than in the e^+e^- collision. Therefore, such a photon-photon collision option is well motivated from the viewpoint of probing new physics.

IV. CONCLUSION

We studied the process $\gamma\gamma \rightarrow h \rightarrow b\bar{b}$ at the photon-photon collision of the ILC as a probe of different little Higgs models, including the SLH, LH, LHT-I and LHT-II. We obtained the following observations: (i) Compared with the SM prediction, the SLH, LH and LHT-I always suppress the rate of $\gamma\gamma \rightarrow h \rightarrow b\bar{b}$; while the LHT-II can either suppress or enhance the rate, depending on the values of the Higgs mass and scale f ; (ii) The deviation of the production rate from its SM prediction is sensitive to the scale f in all these models. In the SLH, the deviation is also sensitive to $\tan\beta$; (iii) The production rates in the SLH and

LHT-I/LHT-II can be severely suppressed in some part of the parameter space where the new decay mode, $h \rightarrow \eta\eta$ for the SLH and $h \rightarrow A_H A_H$ for the LHT-I/LHT-II, is open and dominant. Therefore, the precision measurement of such a production process at the ILC will allow for a test of these models and even distinguish between different scenarios.

Acknowledgment

This work was supported in part by the Foundation of Yantai University under Grant No.WL09B31, by the National Natural Science Foundation of China (NNSFC) under grant Nos. 10821504, 10725526 and 10635030, by the Project of Knowledge Innovation Program (PKIP) of Chinese Academy of Sciences under grant No. KJCX2.YW.W10 and by an invitation fellowship of LHC Physics Focus Group, National Center for Theoretical Sciences, Taiwan, Republic of China.

Appendix A: The Effective couplings of Higgs-photon-photon and Higgs-gluon-gluon

The effective Higgs-photon-photon coupling can be written as [18, 33]

$$\mathcal{L}_{h\gamma\gamma}^{eff} = -\frac{\alpha}{8\pi v} I F_{\mu\nu} F^{\mu\nu} h, \quad (\text{A1})$$

where $F^{\mu\nu}$ is the electromagnetic field strength tensor. With the Higgs boson couplings to the charged fermion f_i , vector boson V_i and scalar S_i given by

$$\mathcal{L} = \sum_{f_i} -\frac{m_{f_i}}{v} y_{f_i} \bar{f}_i f_i h + \sum_{V_i} 2\frac{m_{V_i}^2}{v} y_{V_i} V_i V_i h + \sum_{S_i} -2\frac{m_{S_i}^2}{v} y_{S_i} S_i S_i h, \quad (\text{A2})$$

the factor I in Eq. (A1) can be written as

$$I = \sum_{f_i} Q_{f_i}^2 N_{cf_i} y_{f_i} I_{\frac{1}{2}}(\tau_{f_i}) + \sum_{V_i} Q_{V_i}^2 y_{V_i} I_1(\tau_{V_i}) + \sum_{S_i} Q_{S_i}^2 y_{S_i} I_0(\tau_{S_i}), \quad (\text{A3})$$

where Q_X (X denotes f_i , V_i and S_i) is the electric charge for a particle X running in the loop, and N_{cf_i} is the color factor for f_i . The dimensionless loop factors are

$$I_{\frac{1}{2}}(\tau_{f_i}) = -2\tau_{f_i} [1 + (1 - \tau_{f_i})f(\tau_{f_i})], \quad (\text{A4})$$

$$I_1(\tau_{V_i}) = 2 + 3\tau_{V_i} + 3\tau_{V_i}(2 - \tau_{V_i})f(\tau_{V_i}), \quad (\text{A5})$$

$$I_0(\tau_{S_i}) = \tau_{S_i} [1 - \tau_{S_i}f(\tau_{S_i})], \quad (\text{A6})$$

where $\tau_X = 4m_X^2/m_h^2$ and

$$f(\tau_X) = \begin{cases} [\sin^{-1}(1/\sqrt{\tau_X})]^2, & \tau_X \geq 1 \\ -\frac{1}{4}[\ln(\eta_+/\eta_-) - i\pi]^2, & \tau_X < 1 \end{cases} \quad (\text{A7})$$

with $\eta_{\pm} = 1 \pm \sqrt{1 - \tau_X}$. When the masses of particles in the loops are much larger than half of the Higgs boson mass, we can get

$$I_{\frac{1}{2}}(\tau_{f_i}) \simeq -4/3, \quad I_1(\tau_{V_i}) \simeq 7, \quad I_0(\tau_{S_i}) \simeq -1/3. \quad (\text{A8})$$

The effective Higgs-gluon-gluon coupling can be written as [18, 33]

$$\mathcal{L}_{hgg}^{eff} = -\frac{\alpha_s}{12\pi v} I_{hgg} G_{\mu\nu}^{\alpha} G_{\alpha}^{\mu\nu} h, \quad (\text{A9})$$

where $G_{\mu\nu}^{\alpha} = \partial_{\mu}g_{\nu}^{\alpha} - \partial_{\nu}g_{\mu}^{\alpha}$ and the factor I_{hgg} from the contributions of quarks running in the loops is given by

$$I_{hgg} = \sum_{q_i} \frac{3}{4} y_{q_i} I_{\frac{1}{2}}(\tau_{q_i}), \quad (\text{A10})$$

with $\tau_{q_i} = 4m_{q_i}^2/m_h^2$.

Once the interactions in Eq. (A2) are given, we can obtain the effective $h\gamma\gamma$ and hgg couplings from the above formulas. In the following we list the relevant Higgs interactions in the SLH, LH, LHT-I and LHT-II, respectively. Here the Higgs interactions with the light fermions are not listed since their contributions can be ignored.

(1) In the SLH, the Higgs couplings with the quarks are given by

$$\mathcal{L}_t \simeq -f\lambda_2^t \left[x_{\lambda}^t c_{\beta} t_1^{c'} (-s_1 t_L' + c_1 T_L') + s_{\beta} t_2^{c'} (s_2 t_L' + c_2 T_L') \right] + h.c., \quad (\text{A11})$$

$$\mathcal{L}_d \simeq -f\lambda_2^d \left[x_{\lambda}^d c_{\beta} d_1^{c'} (s_1 d_L' + c_1 D_L') + s_{\beta} d_2^{c'} (-s_2 d_L' + c_2 D_L') \right] + h.c., \quad (\text{A12})$$

$$\mathcal{L}_s \simeq -f\lambda_2^s \left[x_{\lambda}^s c_{\beta} s_1^{c'} (s_1 s_L' + c_1 S_L') + s_{\beta} s_2^{c'} (-s_2 s_L' + c_2 S_L') \right] + h.c., \quad (\text{A13})$$

where

$$s_1 \equiv \sin \frac{t_{\beta}(h+v)}{\sqrt{2}f}, \quad s_2 \equiv \sin \frac{(h+v)}{\sqrt{2}t_{\beta}f}, \quad s_3 \equiv \sin \frac{(h+v)(t_{\beta}^2+1)}{\sqrt{2}t_{\beta}f}. \quad (\text{A14})$$

After diagonalization of the mass matrix in Eqs. (A11), (A12) and (A13), we can get the mass eigenstates (t, T) , (d, D) and (s, S) , which was performed numerically in our analysis, and the relevant couplings with Higgs boson can be obtained without

resort to any expansion of v/f (the diagonalization of the quark mass matrix in the LH, LHT-I and LHT-II was also performed numerically in our calculation).

The Higgs coupling with the bosons is given by [14],

$$\mathcal{L} = 2\frac{m_W^2}{v}y_W W^+W^-h + 2\frac{m_{W'}^2}{v}y_{W'}W'^+W'^-h, \quad (\text{A15})$$

where

$$y_W \simeq \frac{v}{v_{SM}} \left[1 - \frac{v_{SM}^2}{4f^2} \frac{t_\beta^4 - t_\beta^2 + 1}{t_\beta^2} + \frac{v_{SM}^4}{36f^4} \frac{(t_\beta^2 - 1)^2}{t_\beta^2} \right], \quad y_{W'} \simeq -\frac{v^2}{2f^2}. \quad (\text{A16})$$

(2) In the LH, the Higgs couplings with the heavy quarks are given by

$$\mathcal{L}_t \simeq -\lambda_1 f \left[\frac{s_\Sigma}{\sqrt{2}} \bar{u}_L u_R + \frac{1 + c_\Sigma}{2} \bar{U}_L U_R \right] - \lambda_2 f \bar{U}_L U_R + \text{h.c.}, \quad (\text{A17})$$

where $c_\Sigma \equiv \cos \frac{\sqrt{2}(v+h)}{f}$ and $s_\Sigma \equiv \sin \frac{\sqrt{2}(v+h)}{f}$. After diagonalization of the mass matrix in Eq. (A17), we can get the mass eigenstates t and T as well as their couplings with the Higgs boson [18]:

$$\mathcal{L} = -\frac{m_t}{v}y_t \bar{t} t h - \frac{m_T}{v}y_T \bar{T} T h, \quad (\text{A18})$$

where

$$y_t = 1 + \frac{v^2}{f^2} \left[-\frac{2}{3} + \frac{x}{2} - \frac{x^2}{4} + c_t^2 s_t^2 \right], \quad y_T = -c_t^2 s_t^2 \frac{v^2}{f^2}. \quad (\text{A19})$$

The Higgs coupling with the bosons are given by

$$\begin{aligned} \mathcal{L} = & 2\frac{m_W^2}{v}y_W W^+W^-h + 2\frac{m_{W_H}^2}{v}y_{W_H} W_H^+W_H^-h \\ & -2\frac{m_\Phi^2}{v}y_{\Phi^+}\Phi^+\Phi^-h - 2\frac{m_\Phi^2}{v}y_{\Phi^{++}}\Phi^{++}\Phi^{--}h, \end{aligned} \quad (\text{A20})$$

where

$$\begin{aligned} y_{W_L} &= 1 + \frac{v^2}{f^2} \left[-\frac{1}{6} - \frac{1}{4}(c^2 - s^2)^2 \right], \quad y_{W_H} = -s^2 c^2 \frac{v^2}{f^2}, \\ y_{\Phi^+} &= \frac{v^2}{f^2} \left[-\frac{1}{3} + \frac{1}{4}x^2 \right], \quad y_{\Phi^{++}} = \frac{v^2}{f^2} \mathcal{O}\left(\frac{x^2}{16} \frac{v^2}{f^2}, \frac{1}{16\pi^2}\right). \end{aligned} \quad (\text{A21})$$

Since the $h\Phi^{++}\Phi^{--}$ coupling is very small, the contributions of the doubly-charged scalar can be ignored.

(3) In the LHT-I, the Higgs couplings with the heavy quarks are given by

$$\begin{aligned} \mathcal{L}_\kappa \simeq & -\sqrt{2}\kappa f \left[\frac{1 + c_\xi}{2} \bar{u}_{L-} u'_{R-} - \frac{1 - c_\xi}{2} \bar{u}_{L-} q_R - \frac{s_\xi}{\sqrt{2}} \bar{u}_{L-} \chi_R \right] \\ & -m_q \bar{q}_L q_R - m_\chi \bar{\chi}_L \chi_R + \text{h.c.}, \end{aligned} \quad (\text{A22})$$

$$\mathcal{L}_t \simeq -\lambda_1 f \left[\frac{s_\Sigma}{\sqrt{2}} \bar{u}_{L+} u_R + \frac{1+c_\Sigma}{2} \bar{U}_{L+} u_R \right] - \lambda_2 f \bar{U}_{L+} U_{R+} + \text{h.c.}, \quad (\text{A23})$$

where $c_\xi \equiv \cos \frac{v+h}{\sqrt{2}f}$ and $s_\xi \equiv \sin \frac{v+h}{\sqrt{2}f}$. After diagonalization of the mass matrix in Eq. (A22), we can get the T-odd mass eigenstates u_- , q and χ . In fact, there are three generations of T-odd particles, and we assume they are degenerate. The mass eigenstates t and T can be obtained by mixing the interaction eigenstates in Eq. (A23).

The Higgs interactions with the bosons in the LHT-I can be obtained from the couplings in the LH by taking $c = s = 1/\sqrt{2}$ and $x = 0$.

- (4) In the LHT-II, the Higgs couplings with the first two generations of heavy quarks are given by

$$\mathcal{L}_q^{1,2} \simeq -\sqrt{2}\kappa f \left[\frac{1+c_\xi}{2} \bar{u}_{L-} u'_R - \frac{1-c_\xi}{2} \bar{u}_{L-} q_R + \frac{s_\xi}{\sqrt{2}} \bar{u}_{L+} \chi_R \right] - m_q \bar{q}_L q_R - m_\chi \bar{\chi}_L \chi_R + \text{h.c.} \quad (\text{A24})$$

The mass eigenstates of u_- , q and χ can be obtained by the diagonalization of the mass matrix in Eq. (A24).

The Higgs couplings with the third generation of heavy quarks are given by

$$\begin{aligned} \mathcal{L}_q^3 \simeq & -\sqrt{2}\kappa f \left[\frac{1+c_\xi}{2} \bar{u}_{L-} u'_R - \frac{1-c_\xi}{2} \bar{u}_{L-} q_R - \frac{s_\xi}{\sqrt{2}} \bar{U}_{L-} q_R - \frac{s_\xi}{\sqrt{2}} \bar{U}_{L-} u'_R + \frac{s_\xi}{\sqrt{2}} \bar{u}_{L+} \chi_R \right. \\ & \left. + c_\xi \bar{\chi}_L \chi_R \right] - m_q \bar{q}_L q_R - \lambda f \left[s_\Sigma \bar{u}_{L+} u_{R+} + \frac{1+c_\Sigma}{\sqrt{2}} \bar{U}_{L-} U_{R-} \right] + \text{h.c.}, \quad (\text{A25}) \end{aligned}$$

where c_t is taken as $1/\sqrt{2}$. After diagonalization of the mass matrix in Eq. (A25), we can get the mass eigenstates t , T_- , u_- , q and χ .

The Higgs interactions with the bosons in the LHT-II are the same as in the LHT-I.

Note that in the lepton sector, the SLH, LHT-I and LHT-II also predict some neutral heavy neutrinos, which do not contribute to the couplings of $h\gamma\gamma$ and hgg at the one-loop level. Although the charged heavy leptons and down-type T-odd quarks are predicted in LHT-I and LHT-II, they do not have direct couplings with the Higgs boson. Besides, from Eqs. (A1) and (A9), we can find that the effective couplings of $h\gamma\gamma$ and hgg are related to

the Higgs VEV v and the running α and α_s in these models.

-
- [1] N. Arkani-Hamed, A. G. Cohen and H. Georgi, Phys. Lett. B **513**, 232 (2001); N. Arkani-Hamed, *et al.*, JHEP **0208**, 021 (2002).
 - [2] D. E. Kaplan and M. Schmaltz, JHEP **0310**, 039 (2003); I. Low, W. Skiba, and D. Smith, Phys. Rev. D **66**, 072001 (2002); S. Chang and J. G. Wacker, Phys. Rev. D **69**, 035002 (2004); T. Gregoire, D. R. Smith, and J. G. Wacker, Phys. Rev. D **69**, 115008 (2004); W. Skiba and J. Terning, Phys. Rev. D **68**, 075001 (2003); S. Chang, JHEP **0312**, 057 (2003); H. Cai, H.-C. Cheng, and J. Terning, JHEP **0905**, 045 (2009); A. Freitas, P. Schwaller, and D. Wyler, arXiv:0906.1816.
 - [3] N. Arkani-Hamed, A. G. Cohen, E. Katz, A. E. Nelson, JHEP **0207**, 034 (2002).
 - [4] M. Schmaltz, JHEP **0408**, 056 (2004).
 - [5] T. Han, H. E. Logan and L. T. Wang, JHEP **0601**, 099 (2006).
 - [6] C. Csaki, *et al.*, Phys. Rev. D **67**, 115002 (2003); Phys. Rev. D **68**, 035009 (2003); J. L. Hewett, F. J. Petriello, T. G. Rizzo, JHEP **0310**, 062 (2003); M. C. Chen, S. Dawson, Phys. Rev. D **70**, 015003 (2004); M. C. Chen, *et al.*, Mod. Phys. Lett. A **21**, 621 (2006).
 - [7] G. Marandella, C. Schappacher and A. Strumia, Phys. Rev. D **72**, 035014 (2005).
 - [8] A. G. Dias, C. A. de S. Pires, P. S. Rodrigues da Silva, Phys. Rev. D **77**, 055001 (2008).
 - [9] H. C. Cheng and I. Low, JHEP **0309**, 051 (2003).
 - [10] H. C. Cheng and I. Low, JHEP **0408**, 061 (2004); I. Low, JHEP **0410**, 067 (2004).
 - [11] H. C. Cheng, I. Low and L. T. Wang, Phys. Rev. D **74**, 055001 (2006).
 - [12] A. Martin, hep-ph/0602206.
 - [13] G. Cacciapaglia, A. Deandrea, J. Llodra-Perez, JHEP **0906**, 054 (2009).
 - [14] K. Cheung and J. Song, Phys. Rev. D **76**, 035007 (2007).
 - [15] W. Kilian, D. Rainwater and J. Reuter, Phys. Rev. D **71**, 015008 (2005).
 - [16] K. Cheung, *et al.*, Phys. Rev. D **78**, 055015 (2008); Phys. Rev. Lett. **99**, 031801 (2007); X.-F. Han, L. Wang, J. M. Yang, Nucl. Phys. B **825**, 222 (2010).
 - [17] J. J. Liu, *et al.*, Phys. Rev. D **70**, 015001 (2004); A. Gonzalez-Sprinberg, R. Martinez, J. Rodriguez, Phys. Rev. D **71**, 035003 (2005); S. Yang, arXiv:0904.1646.
 - [18] T. Han, H. E. Logan, B. McElrath, L.-T. Wang, Phys. Lett. B **563**, 191 (2003) [Erratum-ibid.

- B 603, 257 (2004)].
- [19] C. R. Chen, K. Tobe, C. P. Yuan, Phys. Lett. B **640**, 263 (2006).
 - [20] K. Hsieh, C. P. Yuan, Phys. Rev. D **78**, 053006 (2008); C. O. Dib, R. Rosenfeld, A. Zerwekh, JHEP **0605**, 074 (2006); R. S. Hundi, B. Mukhopadhyaya, A. Nyffeler, Phys. Lett. B **649**, 280 (2007); X. F. Han, L. Wang, J. M. Yang, Phys. Rev. D **78**, 075017 (2008); L. Wang, *et al.*, Phys. Rev. D **76**, 017702 (2007); Phys. Rev. D **75**, 074006 (2007); M. Asano, S. Matsumoto, N. Okada and Y. Okada, Phys. Rev. D **75**, (2007) 063506; C.-X. Yue, *et al.*, Chin. Phys. Lett. **25**, 66 (2008).
 - [21] L. Wang, J. M. Yang, Phys. Rev. D **77**, 015020 (2008); Phys. Rev. D **79**, 055013 (2009).
 - [22] D. Zeppenfeld, R. Kinnunen, A. Nikitenko and E. Richter-Was, Phys. Rev. D **62**, 013009 (2000); A. Djouadi *et al.*, hep-ph/0002258; A. Belyaev and L. Reina, JHEP **0208**, 041 (2002); M. Dührssen, ATL-PHYS-2003-030; M. Dührssen, S. Heinemeyer, H. Logan, D. Rainwater, G. Weiglein and D. Zeppenfeld, hep-ph/0406323.
 - [23] G. Jikia and S. Soldner-Rembold, Nucl. Phys. Proc. Suppl. **82**, 373 (2000); Nucl. Instrum. Meth. A **472**, 133 (2001); P. Niezurawski, A. F. Zarnecki, M. Krawczyk, Acta Phys. Polon. B **34**, 177 (2003); A. Rosca and K. Monig, hep-ph/0310036.
 - [24] P. Niezurawski, A. F. Zarnecki and M. Krawczyk, hep-ph/0307183.
 - [25] H. E. Logan, Phys. Rev. D **70**, 115003 (2004).
 - [26] T. Han, H. E. Logan, B. McElrath, L.-T. Wang, Phys. Rev. D **67**, 095004 (2003).
 - [27] J. Hubisz and P. Meade, Phys. Rev. D **71**, 035016 (2005).
 - [28] O. J. P. Eholi, *et al.*, Phys. Rev. D **47**, 1889 (1993); K. Cheung, Phys. Rev. D **47**, 3750 (1993).
 - [29] J. Hubisz, P. Meade, A. Noble, M. Perelstein, JHEP **0601**, 135 (2006).
 - [30] C. Amsler, *et al.*, Phys. Lett. B **667**, 1 (2008).
 - [31] A. Djouadj, J. Kalinowski and M. Spira, Computl. Phys. Commun. **108**, 56 (2006).
 - [32] See, e.g., J. Cao, *et al.*, Nucl. Phys. B **651**, 87 (2003); Eur. Phys. Jour. C **41**, 381 (2005); Phys. Rev. D **58**, 094004 (1998).
 - [33] J. F. Gunion, H. E. Haber, G. L. Kane, and S. Dawson, "The Higgs Hunters Guide," Addison-Wesley, Reading, MA (1990).